Solid–Liquid–Vapor Equilibrium Models for Cryogenic Biogas Upgrading

Riva Mauro, Marco Campestrini, Joseph Toubassy, Denis Clodic, Paolo Stringari

Solid-Liquid-Vapor Equilibrium Models for Cryogenic Biogas Upgrading

Mauro Riva [a,b], Marco Campestrini [a], Jouseph Toubassy [b], Denis Clodic [b], Paolo Stringari [a,*],

[a] *MINES ParisTech - PSL Research University - CTP, Center Thermodynamics of Processes, 35 rue Saint Honoré, 77305 Fontainebleau Cedex, France.*

[b] *EReIE, 3 rue de la Croix Martre, 91120 Palaiseau, France.*

* Corresponding author. Tel.: +33 (0)1 64 69 48 57. E-mail address: paolo.stringari@mines-paristech.fr

Abstract

Design and optimization of cryogenic technologies for biogas upgrading require accurate determination of freeze out boundaries. In cryogenic upgrading processes involving dry ice formation, accurate predictions of solid-liquid, solid-vapor, and solid-liquid-vapor equilibria are fundamental for a correct design of the heat exchanger surface in order to achieve the desired biomethane purity. Moreover, Liquefied BioGas production process, particularly interesting for cryogenic upgrading processes due to the low temperature of the obtained biomethane, requires an accurate knowledge of carbon dioxide solubility in liquid methane to avoid solid deposition.

The present work compares two different approaches for representing solid-liquid, solid-vapor, and solid-liquid-vapor equilibria. The first approach consists in using a cubic equation of state coupled with a solid phase fugacity expression. In the second approach, a single equation of state representing solid, liquid, and vapor phases is used. Binary interaction parameters for both the models have been regressed in order to optimize the representation of phase equilibrium at low temperatures, with particular emphasis to the equilibria involving a solid phase. The two models, with the same number of adjustable parameters, give equivalent representations of solid-liquid, solid-vapor, and solid-liquid-vapor equilibria. The comparison with experimental data shows that these models are adapted for an accurate representation of the CH_4-CO_2 mixture behavior at low temperatures. Furthermore, an extended bibliographic research on experimental data on phase equilibrium involving solid phase and the comparison with results obtained from two allow determining the regions where more accurate data are needed.

Keywords: biogas upgrading, biomethane, cryogenic processes, equation of state, liquefied biogas, solid-liquid-vapor equilibrium.

1. Introduction

Increasing trend of oil and natural gas prices and new targets for renewable fuels quotes lead to an increasing interest on the use of biogas as alternative source of energy. Biogas is produced by the anaerobic digestion of organic substrate, which can come from recycled material like agricultural wastes, manure and industrial wastewater. Raw biogas consists mainly of methane (CH_4) and carbon dioxide (CO_2), along with water and traces of pollutants such as hydrogen sulphide, ammonia and particulates. The raw biogas is then purified to prevent corrosion and mechanical wear of the equipments in which it is used. For some applications demanding a high energy content gas, namely vehicle fuels and injection in the natural gas grid, the biogas has to be upgraded into biomethane. It means that the concentration of methane in the biogas must be increased by removing carbon dioxide.

According to the information published by IEA Bioenergy Task 37 (1), 347 upgrading plants are operating worldwide at the time the article is written. The most used technologies in biogas upgrading are: water scrubbers (115 plants), pressure swing adsorption units, alone or coupled with water scrubbers or membranes (72 plants), chemical scrubbers (69 plants), membrane units (22 plants) and organic physical scrubbers (17 plants). An innovative technology is the CO_2 cryogenic separation, which is still not well established in the market (only one plant is operating according to the IEA), mainly because of the high expected cooling cost. Nevertheless it is in continuous development thanks to interesting advantages. In fact no absorbents are required and CO_2 can be captured at atmospheric pressure instead of high operating pressure needed for the

other technologies. Another important advantage is the very low methane slip (the methane lost with the removed CO_2) compared with other technologies (2).

With these advantages, the research on cryogenic CO_2 capture technologies has made significant progresses in the last 10 years. Cryogenic processes working at atmospheric pressure have to deal with freeze out of CO_2 directly from the vapor phase, because of its high triple point. Researches in this field result in the development of different processes. For instance, Tuinier et al. (3) exploited a novel cryogenic capture process using dynamically operated packed beds, whereas Song et al. (4) and Chang et al. (5) developed two cryogenic separating systems able to capture the CO_2 for solidification in heat exchangers. The adopted refrigerating systems are a Stirling chiller (4) and a Brayton refrigerator (5), respectively. In 2001, Clodic and Younes (6) developed a cryogenic separation process, in which the CO_2 could be captured as a solid on the fins of heat exchangers which were cooled thanks to an Integrated Cascade system. This solution allows lower energy consumption (7), and it has been later developed by the company EReIE leading to the CRYO-PUR® technology (8). This system is able to produce both biomethane as Compressed Natural Gas (CNG) for injection in natural gas grid or as fuel vehicle, and Liquefied Biomethane. This second option is, like for the Liquefied Natural Gas (LNG), interesting for trucks fuelling and for optimizing biomethane transportation and distribution. In the cryogenic capture technology, the operative temperature in the heat exchanger ranges, depending on the required upgrading level, between 140 K and the normal CO_2 sublimation temperature, around 200 K. In case of liquefaction of the biomethane, the operating pressure is up to 1.5 MPa.

Upgrading of biogas generates new possibilities for its use since it can replace natural gas, meeting, in terms of Lower Heating Power and CO_2 concentration, the standards for the injection in the natural gas grid or for its use as vehicle fuel. On the other hand, the upgrading process adds

costs to the biogas production. It is then important to have an optimized upgrading process in terms of low energy consumption and high methane content in the upgraded biogas. Moreover, for a cryogenic process, energy efficiency in reaching low temperatures is fundamental to be competitive with the other technologies. For the design of the cryogenic upgrading process, a model to estimate the properties of the biogas, which can be preliminarily assumed as a binary mixture of methane and carbon dioxide, is necessary. Since the process takes advantages from solid formation to capture and separate the carbon dioxide, the model has to dial with phase equilibrium occurring between the solid and the fluid phases, namely solid-vapor, solid-liquid and solid-liquid-vapor equilibrium.

In this work, two different approaches for representing the phase equilibrium of methane-carbon dioxide have been compared. The first approach consists in using an equation of state (EoS) for representing the fugacity of the fluid phases, and an independent model for the fugacity of the solid phase, see for instance Prausnitz et al. (9). The second approach is based on an EoS capable of representing solid, liquid, and vapor phases at the same time (10). Binary interaction parameters have been regressed for both the models in order to optimize the representation of the available experimental data of solid-liquid, solid-vapor, and solid-liquid-vapor equilibrium.

2. Experimental values for the system CH_4-CO_2: literature review

The triple point and critical point temperatures and pressures for CH_4 and CO_2 have been obtained from the NIST Standard Reference Database 23, version 8.0 (11), and resumed in Tab. 1.

Experimental values concerning the solid-liquid equilibrium (SLE), the solid-vapor equilibrium (SVE), and the solid-liquid-vapor equilibrium (SLVE) have been proposed by several authors

since the 1950s (12-26). Taking into account these works and the corresponding data, one can state at once that the solid phase is usually considered as composed by pure CO_2. Furthermore, because no experimental values for the CH_4-CO_2 mixture are available under 97 K, it follows that the mixture phase equilibrium behavior is still not well identified for temperatures lower than the pure CH_4 triple point temperature. For these temperatures also methane solidifies, thus giving a second solid phase in equilibrium with the pure solid CO_2. According to that, it can be stated that the mixture presents immiscibility in the solid phase. As a consequence, the mixture should present a quadruple point, where a liquid, a vapor, and two solid phases coexist at equilibrium for appropriate values of pressure and temperature. In dealing with the presence of two solid phases, let's consider the subscript 1 for referring to the solid phase rich in methane, while using the subscript 2 for the pure solid carbon dioxide.

Even though the quadruple point has not been experimentally measured yet, a precious support in confirming this feature and in understanding the global phase equilibrium behavior of the mixture has been provided by Donnelly and Katz in 1954 (12). These authors obtained experimental results concerning the mixture critical locus, the vapor-liquid equilibrium (VLE), the S_2LVE and the S_2LE. Same authors extrapolated the fluid phase compositions along the S_2LVE locus toward an eutectic point, which corresponds to having a quadruple point temperature lower than the pure CH_4 triple point temperature.

As previously stated, the temperature range of interest for the cryogenic separation process extends from around 140 K up to 200 K. Concerning the pressure, the process works at atmospheric pressure and values up to 1.5 MPa can be reached in case of liquefaction of biomethane. Nevertheless, authors of this work have considered all the available experimental values involving the pure CO_2 solid phase, S_2 (12-26).

Considering the presence of a quadruple point, the pressure-temperature equilibrium behavior of the binary mixture methane-carbon dioxide can be qualitatively illustrated in Fig. 1. The abbreviations used in Fig .1 for indicating the different kind of phase equilibria and their meaning are listed in Tab. 2.

In Fig. 1, the vapor-liquid critical locus exits the pure CH_4 critical point extending continuously toward the CO_2 critical point. This feature is endorsed by experimental values reported for instance in Donnelly and Katz (12). With reference to lines where three phases coexist at equilibrium, four triple point loci can be identified. These four triple point loci join together in the quadruple point, indicated by a black triangle in Fig. 1. The $s_2$lve and the $s_1$lve originating from this point end in the triple point of pure CO_2 and CH_4, respectively, while the $s_2s_1$ve extends down to the low temperature region. The remaining triple point locus, the $s_2s_1$le locus, extends to the high pressure region. A zoom of the phase equilibrium behavior in the pressure-temperature region close to the pure CH_4 triple point has been added in Fig. 1, and it details the four triple point loci and the quadruple point. The quadruple point has been placed at a temperature and a pressure lower than the corresponding values of the CH_4 triple point, as suggested by Donnelly and Katz (12).

Tab. 3 presents a review of SLVE, SLE and SVE data proposed by different authors (12-26), specifying the corresponding type of equilibrium, the number of experimental values (NEV), and their temperature, pressure, and CO_2 molar fraction ranges. Considering that this work does not deal with temperatures lower than the CH_4 triple point temperature and that all the experimental values involve only the pure CO_2 solid phase, a distinction between solid phases S_1 and S_2 is

useless in this context. As a consequence, unless otherwise stated, S is henceforth used for indicating the sole solid phase occurring for temperature greater than the CH_4 triple point.

In 1954, Donnelly and Katz (12) provided SLE and SLVE data in the range from 194.54 K to 215.37 K. Sterner in 1961 (13) extended the work of Donnelly and Katz to temperatures down to 166.48 K for the SLVE. Data on the SLVE curve and solid-liquid equilibrium have been provided for a wide range of conditions by Davis in 1962 (14). In 1971, Im and Kurata (15) reported an experimental study of the vapor and liquid compositions at multiphase equilibrium of light paraffins in presence of solid CO_2. The authors report data along the SLVE locus of the binary CO_2-CH_4 mixture in the range of temperature from 165.21 to 210.21 K and pressure between 1.9 and 4.85 MPa. Further measurements on the solid-liquid equilibrium have been done by Brewer and Kurata in 1958 (16) for a range of temperature similar to the one studied by Donnelly and Katz (12). Different authors, (17), (18), (19) and (20), provided experimental data for the SLE of the methane and carbon dioxide mixtures at temperature down to 110 K. Recently Shen et al. (21) and Gao et al. (22) measured the SLE in the range of temperature between 112 and 170 K.

In 1959 Pikaar (23) investigated the CH_4-CO_2 system in particular in the solid-vapor region for temperature down to 130 K, reporting a great amount of data obtained with two different experimental techniques (constant volume cell apparatus and saturation cell apparatus). A second set of data in the solid-vapor region for the CO_2-CH_4 mixture has been measured by Agrawall and Leverman in 1974 in the range of condition of interest for the LNG industry (24). Recently Le and Trebble studied the methane-carbon dioxide mixture at the solid-vapor equilibrium in a range of temperature from 168 to 187 K (25). In 2011 new experimental data are reported by

Zhang et al. (26) for the frost points of the CO_2-CH_4 systems for a wide range of CO_2 compositions (i.e., CO_2 mole fraction from 0.108 to 0.542).

3. Thermodynamic models for SVE, SLE, and SLVE of the CH_4-CO_2 mixture

In a mixture of *N* components, the equilibrium condition between two phases α and β is written in terms of fugacity as:

$$\hat{f}_i^{\alpha}(T, P, x^{\alpha}) = \hat{f}_i^{\beta}(T, P, x^{\beta}) \quad (1)$$

or, in terms of activity coefficients:

$$x_i^{\alpha}\gamma_i^{\alpha}(T, P, x^{\alpha}) = x_i^{\beta}\gamma_i^{\beta}(T, P, x^{\beta}) \quad (2)$$

Eqs. (1) and (2) must apply to all the *N* components in the mixture. In Eqs. (1) and (2), $\hat{f}_i$ and γ_i are the partial molar fugacity and the activity coefficient of the component *i* in phase α or β, while *x* is the composition in each phase. As stated above, in this work the biogas is considered to be a binary mixture of methane and carbon dioxide. Subscripts 1 and 2 are used in Eq. (1) for indicating methane and carbon dioxide, respectively, and subscripts S, L, and V refer to the solid, the liquid, and the vapor phase, respectively. Eqs. (1) and (2) can then be applied to the SVE, the SLE, and the VLE.

At the SLVE, three phases coexist, so the equilibrium condition in terms of fugacity can be written as:

$$\hat{f}_i^{S}(T, P, x) = \hat{f}_i^{L}(T, P, x) = \hat{f}_i^{V}(T, P, x) \quad (3)$$

for i = 1, 2. In this work, two different approaches are compared to calculate the fugacities (or,

equivalently, the activity coefficients) of each phase at equilibrium. The former consists in using a cubic Equation of State (EoS) for representing the fluid phase fugacities, while solid fugacities are evaluated from a specific solid fugacity model.

The latter model uses an unique EoS for representing solid, liquid, and vapor phases, and corresponds to the EoS proposed by Yokozeki in 2003 (10). In the following part of this work, the first approach will be referred to as Model 1, the second one as Model 2.

3.1 Model 1

Model 1 couples the Peng Robinson (PR) EoS, with Van der Waals mixing rules, and an independent model for the solid phase fugacity.

The application of the PR EoS in representing phase equilibria involving fluid phases is common knowledge, therefore this work focuses on the SLE, SVE, and SLVE. Frequently adopted literature approaches propose different expressions for the calculation of solid fugacity in SLE and SVE. In both cases the solid phase is assumed composed only by the heavy compound, CO_2. A supplementary discussion is presented with reference to the application of a SLE model coupled with a SVE model for the representation of the SLVE.

Solid-Liquid Equilibrium

As demonstrated by Prausnitz et al. (9), if the solid phase is considered as composed of pure CO_2, the SLE condition can be written as in Eq. (4):

$$\ln x_2^L \gamma_2^L = -\frac{\Delta h_{FUS}}{RT_t}\left(\frac{T_t}{T}-1\right)+\frac{\Delta c_p}{R}\left(\frac{T_t}{T}-1\right)-\frac{\Delta c_p}{R}\ln\frac{T_t}{T} \qquad (4)$$

In Eq. (4), x_2^L is the solubility (mole fraction) of CO_2, γ_2^L is the liquid phase activity coefficient, while Δh_{FUS} and T_t are enthalpy of fusion and triple point temperature of CO_2, respectively. The value of the activity coefficient is derived from the PR EoS.

Solid-Vapor Equilibrium

Assuming the solid phase as pure CO_2, the solid phase fugacity can be related to the fugacity of the saturated vapor at the temperature of the system and the sublimation pressure through the Poynting factor, thus Eq. (1) can be rewritten in terms of fugacity coefficients as (9):

$$x_2^V \hat{\varphi}_2^V P = P_2^{sat} \varphi_2^{sat} \exp\left[\frac{v_2^S \left(P - P_2^{sat}\right)}{RT}\right] \quad (5)$$

In Eq. (5), the left side corresponds to the CO_2 fugacity in the vapor phase, expressed in terms of CO_2 mole fraction, x_2^V, and the partial molar fugacity coefficient, $\hat{\varphi}_2^V$, which is evaluated from the PR EoS. The right side of Eq. (5) contains the fugacity coefficient of CO_2 at the sublimation pressure φ_2^{sat}, and the solid molar volume v_2^S; other terms are the pressure P, the temperature T, and the gas constant R. It should be kept in mind that Eq. (5) has been obtained assuming the solid molar volume as not pressure dependent. Furthermore, to a fair approximation, the fugacity coefficient of CO_2 at sublimation pressure, φ_2^{sat}, can be assumed equal to unity because P_2^{sat} is small. Concerning P_2^{sat}, in this work authors adopted the sublimation auxiliary equation implemented in REFPROP 8.0 by NIST [11], Eq. (6), to estimate the SVE pressure of CO_2. Knowing the values of the CO_2 triple point temperature and pressure, P_t and T_t, P_2^{sat} can be evaluated as a function of the system temperature T, Eq. (6.)

$$P^{sat} = P_t \exp\left(\frac{T_t}{T}\right)\left[n_1\left(1-\frac{T}{T_t}\right)^{e_1} + n_2\left(1-\frac{T}{T_t}\right)^{e_2} + n_3\left(1-\frac{T}{T_t}\right)^{e_3}\right] \quad (6)$$

The values of parameters n_1, n_2, n_3, e_1, e_2, e_3 of Eq. (6) are given in Tab. 4 (11).

Solid-Liquid-Vapor Equilibrium

The equilibrium among three phases, one of which is solid, is now considered. From the Gibbs rule it is known that for a two component and three phase system, there is one degree of freedom. It means that if pressure is chosen, composition and temperature will be determined by solving Eq. (3), namely the system of two equations among Eq. (1) applied for the SLE, which can be written as Eq. (4), Eq. (1) applied for the SVE, which can be written as Eq. (5), and Eq. (1) applied for the VLE.

Because the fugacity of the solid phase is written in two different ways in the two equations, it results inconsistent to combine Eq. (4) and Eq. (5) for solving the SLE and the SVE when a SLVE occurs. In fact, the fugacity of the solid phase at the same *T* and *P* has a different value if calculated from Eq. (4) or Eq. (5). It is so impossible to find a solution for the system of three equations resumed in Eq. (1). This is clearly shown in the temperature-composition equilibrium behavior for the system methane-carbon dioxide at 1.5 MPa, Fig. 2. When at triple point temperature, vapor and liquid phase compositions are found solving SVE and VLE equations at given pressure, at the same temperature and pressure the SLE condition, given by Eq. (4), provides a different composition of the liquid phase.

Consistent solid fugacity model

As a consequence of the inconsistencies pointed out in the previous section, a unique expression

for the solid phase fugacity for SLE and SVE equilibria is needed. Zabaloy et al. (27) proposed to express the fugacity of the solid phase starting from the fugacity of the liquid phase of the pure component, at same temperature and pressure, Eq. (7):

$$f_2^S(T, v_0) = f_2^L(T, 1, v_0)\exp(U) \tag{7}$$

where v_0 is the molar volume of the pure component 2 (carbon dioxide) in the hypothetical subcooled liquid state at T and P. The fugacity of the pure liquid is evaluated at x_2=1 and v=v_0. The exponential factor *exp(U)* relates the liquid state fugacity with the solid state fugacity for a pure substance at given temperature and pressure.

$$U(T,P) = \frac{\Delta v^{S-L}}{RT}\left[C_1\left(1-\frac{T_t}{T}\right) + C_2\left(\frac{T_t}{T} - 1 + \ln\frac{T}{T_t}\right) + C_3\left(\frac{T}{2T_t} - 1 + \frac{T_t}{2T}\right) + \frac{T_t}{T}\left(P - P_t\right)\right] \tag{8}$$

T_t, P_t, Δv^{S-L} are the triple point temperature, the triple point pressure, and the solid–liquid molar volume difference $(v^S\text{-}v^L)$ of CO_2. Δv^{S-L} is considered constant with temperature and pressure. Parameters C_1, C_2 and C_3 have been obtained by regression on (P, T) values along the pure CO_2 SLE curve obtained from (11).

3.2 Model 2

In 2003, Yokozeki proposed a unique equation of state for representing solid, liquid, and vapor phases (10). The functional form of this pressure explicit equation is reported in Eq. (9).

$$P(T,v) = \frac{RT}{v-b}\frac{v-d}{v-c} - \frac{a}{v^2} \tag{9}$$

In Eq. (9), P is the pressure, R is the gas constant, T is the temperature, v is the molar volume, c is the liquid covolume, b is the solid covolume, a is the parameter keeping into account the

attractive forces among molecules, and *d* represents the volume for which the repulsive term in Eq. (9) is null. The parameters *a* and *b* are functions of temperature, and their functional forms have been presented in (10). Furthermore, this equation can be extended to mixtures thanks to quadratic mixing rules containing a total of four binary interaction parameters (28).

The ability of the Yokozeki EoS with null binary interaction parameters in predicting phase equilibria of binary Lennard-Jones mixtures including solid phases has been tested in (29). That work underlined the necessity to regress the binary interaction parameters on experimental values to make Eq. (9) able of representing different types of solid-fluid equilibria, like solid-liquid azeotrope and eutectic with partial or total immiscibility. In (30), the Yokozeki EoS has been deeply studied, and results have been presented for mixtures of light hydrocarbons and carbon dioxide. In (30), authors proposed regressed binary interaction parameters and compared experimental values for the CH_4-CO_2 system with values calculated with Eq. (9).

4. **Results and discussion**

The values of the regressed parameters for Eq. (8) of Model 1 are reported in Tab. 5. It is worth remembering that these values have been regressed on SLE data of pure CO_2 obtained from (11).

Binary interaction parameters regressed for Model 1 and 2 are presented in Tab. 6. For Model 1, the binary interaction paramenter, k_{ij}, of the van der Waals mixing rules has been regressed on Davis' SLVE data, (14), minimizing an objective function f_{ob} evalueted as the avarage of the squared relative error between experimental and calculated triple point temperature (see Eq. 10).

$$f_{ob} = \frac{1}{N}\sum_{i=1}^{N}\left(\frac{T_i^{calc} - T_i^{\exp}}{T_i^{\exp}}\right)^2 \qquad (10)$$

For Model 2, binary inreraction parameters are taken from Reference 30. In (30), only k_{ij} has been used as binary interaction pareameter, and $l_{ij} = m_{ij} = n_{ij} = 0$. The value of k_{ij} in (30) has been regressed for representing solid-liquid, solid-liquid-vapor, and liquid-vapor equilibria for the CH_4-CO_2 system. For further details on the regression procedure, the reader is invited to see Reference 30.

The capability of Model 1 and Model 2 in representing phase equilibrium literature data for the CH_4-CO_2 system has been evaluated with reference to the following statistical indexes (for the generic property M):

$$AAD = \frac{1}{N}\sum_{i=1}^{N} abs\left(\frac{M_i^{calc} - M_i^{exp}}{M_i^{exp}}\right) \tag{11}$$

$$Bias = \frac{1}{N}\sum_{i=1}^{N} \frac{M_i^{calc} - M_i^{exp}}{M_i^{exp}} \tag{12}$$

$$MAD = \max\left(AAD\right) \tag{13}$$

In Eqs. (11)-(13), N is the number of experimental values.

The comparison between Models 1 and 2 and the experimental data in Tab. 3 are presented in Tabs. 7 to 11 and Figs. 3 to 6. Fig. 3 presents calculated and experimental SLVE and SVE values. For sake of clarity, in this figure only SVE data obtained at constant vapor composition have been considered. From Fig. 3 it can be noticed that the pressure-temperature equilibrium behavior of the triple point locus predicted by the two Models is in good agreement with the experimental

data, even though a mismatch clearly appears with reference to the data of Donnelly and Katz. In particular, for each temperature lower than the temperature of the maximum SLVE pressure, the two models give a higher SLVE pressure than the experimental values of Donnelly and Katz. Furthermore, Model 1 provides a maximum pressure of the triple point curve higher than the corresponding values obtained with Model 2, even if the maximum occurs at about the same temperature value. Table 7 presents the quantitative comparision between SLVE values from literature and values calculated by the two models. More precisely, Tab. 7 shows the values of AAD, Bias and MAD obtained calculating SLV equilibrium pressure at fixed temperature.

According to Tab. 7, it is worth noticing that both models are in a good quantitative agreement with SLVE experimental values, except for the data of Donnelly and Katz (12). As previously stated, data reported in (12) are not consistent with the other experimental values. This inconsistency can be also observed in the AAD, Bias, and MAD% values in Tab. 7. Both models have AAD around 13% for the data of Donnelly and Katz (12), while the AAD is around 2% for the three other series of data (13-15). In the overall line of Tab. 7, the AAD and Bias values are weighted means among the experimental values, while the maximum values of MAD among the different references have been reported.

Concerning the SVE, both models are qualitatively in agreement with Agrawal's constant composition data, as shown in Fig. 3. Results of the comparison among SVE data and Models 1 and 2 are presented in Tabs. 8 and 9. In Tab. 8, AAD, Bias, and MAD% for SVE temperatures have been calculated at fixed pressure and CO_2 molar fraction, while in Tab. 9 AAD, Bias, and MAD% for CO_2 molar fractions have been calculated at fixed pressure and temperature. The comparison of Model 1 and 2 with the data from Le and Trebble (25) shows higher deviations than the others SVE data. In Fig. 4 data from Le and Trebble (25), which are not shown in Fig. 3

for the sake of graphical readability, are compared with results from Models 1 and 2 and data from Pikaar (23) and Agrawall (24). The figure confirms that Models are qualitatively in good agreement with Agrawall's data, while Pikaar (23) and Le and Trebble (25) experimentaly found the solid-vapor equilibrium at higher temperature for the same composition and pressure. Le and Treblle's data at x_{CO2} = 0.01 are even closer to the calculated SVE points at x_{CO2} = 0.02. However, some inconcistency should be present in the set of data from Le and Trebble (25), because at around 174 K and 1.3 MPa they found SVE for mixture with both x_{CO2}=0.01 and x_{CO2}=0.02. Good consistency between the Models and the data from Pikaar (23) is shown in Fig. 5. Among the data measured by Pikaar (23), in Fig. 5 only the data at constant temperature are considered for allowing a graphical comparison with the Models. The performance of the Models with respect to all the data available in Pikaar (23) is evaluated in Tabs. 8 and 9. As it can be observed in Tab. 8, when SVE temperature is calculated at fixed pressure and CO_2 molar fraction, both the models have AAD around 1%, with a better Bias value for Model 2. MAD values are lower than 4% for Model 1 and 3% for Model 2.

When CO_2 molar fractions are calculated at fixed pressure and temperature (see Tab. 9), AAD are about 15% for both the models, with slightly lower value for Model 2. Model 2 presents also a better value of Bias, 2.63%, showing the low sistematic shifting with respect to the data (see Tab. 9). For both the models, the highest deviations are shown with respect to the data of Le and Trebble (25).

Fig. 6 and Tabs. 10 and 11 present the comparison among the SLE calculated from Model 1 and 2 and the literature data. In Tab. 10, AAD, Bias, and MAD% for SLE temperatures have been calculated at fixed CO_2 molar fraction, while in Tab. 10 AAD, Bias, and MAD% for CO_2 molar

fractions have been calculated at fixed temperature. Because few authors report the experimental pressures corresponding to the SLE data, calculations have been carried out at the pressure of the triple point curve corresponding to the temperature (or composition) of the data. From the bibliographic research on experimental data on phase equilibrium involving the solid phase, it is possible to conclude that SLE pressure data are rarely reported. Shen et al. (21), give temperature, pressure and composition of the liquid phase at the SLE. In this case it is possible to observe (see Fig. 3) that the pressure at which data are measured is very close to calculated SLVE pressure. In some cases, SLVE data reporting temperature and liquid phase composition (but not pressure) are considered as SLE data, like for data from Davis (13) in this paper and in Eggeman and Chafin paper (31) and data from Sterner (14) in this paper.

The models are consistent in calculating the solid formation temperature for a fixed composition of the liquid phase. According to the overall line in Tab. 10, the AAD averaged with respect to all the experimental values is less then 2%, and the Bias is -1.08% for Model 1 and -1.36% for Model 2. The maximum absolute deviation is about 4.7% for Model 1 and about 5.2% for Model 2, corresponding to 5.3 K and 8.7 K respectevely. These MAD values correspond to the data of Gao et al. (22) at x_{CO2} = 0.000172 and Sterner (13) at x_{CO2} = 0.019 for Model 1 and 2, respectively.

Quite high values of AAD, Bias and MAD% for CO_2 molar fraction calculated at the SLE for fixed temperature are reported in Tab. 11 for both Model 1 and 2. These high values are caused by the percentage deviations calculated at low temperatures, where CO_2 mole fractions (at denominator) have very low values.

Results show that Model 1 gives a slightly better representation of SLE temperatures calculated at fixed CO_2 molar fraction, while Model 2 allows a slightly better representation of CO_2 molar fractions calculated at fixed temperature.

5. Conclusions

Two different modeling techniques have been compared for the representation of SLVE, SLE, and SVE data of the CH_4-CO_2 mixture. Regressed binary interaction parameters allow a satisfactory representation of the literature data in the considered (*T, P*) range. Both the models need only one, non temperature-dependent, binary interaction parameter. Concerning SLVE data, Model 1 and 2 have comparable AAD and Bias values for the representation of the triple point pressure at fixed temperature. SLVE data from Donnelly and Katz (12) are clearly not consistent with the other SLVE data. Data from Davis et al. (14) and Im and Kurata (15) seem giving the most consistent representation of the SLVE curve for the CH_4-CO_2 mixture. With respect to these data, both the models 1 and 2 overhestimate the maximum pressure of the triple point curve, with slightly lower deviation with respect to the experimental values for Model 2.

For SLE, Model 1 gives slightly better representation of SLE temperature calculated at fixed CO_2 mole fraction, while Model 2 is slightly better in calculating CO_2 mole fraction at fixed temperature. Model 2 performs slightly better also for the representation of SVE. In the authors' opinion, both the models can be safely used in the process simulation of cryogenic biogas upgrading.

Phase equilibrium experimental data for the methane-carbon dioxide system cover a wide range of temperature and pressure, but because of the inconsistency of some SLVE data at temperatures

corresponding to the maximum SLVE pressure, further measurement could be done. It would also result interesting to have more experimental data for the SVE equilibrium in the low CO_2 composition region, corresponding to the range of condition of the process (140-190K), since available SVE data in this region present quite important deviation.

Nomenclature

List of symbols

a	Yokozeki equation of state parameter
b	solid covolume [m^3/mol]
c	liquid covolume [m^3/mol]
C_1	parameters in Eq. (8)
C_2	parameters in Eq. (8)
C_3	parameters in Eq. (8)
d	Yokozeki equation of state parameter
e_1	parameters in Eq. (6)
e_2	parameters in Eq. (6)
e_3	parameters in Eq. (6)
f	fugacity
f_{ob}	objective function
k	binary interaction parameter
l	binary interaction parameter (Yokozeki equation of state)
m	binary interaction parameter (Yokozeki equation of state)

n	binary interaction parameter (Yokozeki equation of state)
n_1	parameters in Eq. (6)
n_2	parameters in Eq. (6)
n_3	parameters in Eq. (6)
x	mole fraction
P	pressure [Pa]
R	gas constant [J/(mol·K)]
T	Temperature [K]
U	parameter in Eq. (7)
v	molar volume [m^3/mol]
Greek letters	
γ	activity coefficients
φ	fugacity coefficients
Subscript	
1	relative to the CH_4
2	relative to the CO_2
c	relative to the critical point
i	relative to the substance *i*
ij	relative to the interaction between substance *i* and the substance *j*
t	related to the triple point
Superscript	
^	relative to a component in a mixture
calc	relative to calculated points
exp	relative to experimental points

sat	relative to saturation condition
α	relative to the phase α
β	relative to the phase β
S	relative to the solid phase
L	relative to the liquid phase
V	relative to the vapor phase

References

(1) IEA Bioenergy Task 37 Up-grading Plant List, *www.iea-biogas.net*, Accessed **2014** May, 21st.

(2) Bauer, F.; Hulteberg, C.; Persson, T.; Tamm, D. SCG Rapport **2013**, 270.

(3) Tuinier, M. J.; van Sint Annaland, M.; Kuipers; J. A. M. *Int. J. Greenh. Gas Control.* **2011**, *5*, 694‑701.

(4) Song, C. F.; Kitamura Y.; Li S. H.; Ogasawara K. *Int. J. Greenh. Gas Control.* **2012**, 7, 107‑114.

(5) Chang, H. M.; Chung, M. J.; Park, S. B. *Adv. Cryog. Eng. AIP Conference Proceedings* **2010**, *1218*, 278-285.

(6) Clodic, D.; Younes, M. *Greenh. Gas Control. Technol. - 6th International Conference* **2003**, 155‑160.

(7) Pan, X.; Clodic, D., Toubassy, J. *Greenhouse Gases Sci. Technol.* **2013**, *3*, 8‑20.

(8) EReIE CRYO-PUR® Project, *www.ereie-sas.fr/technologies.php?id=15*, Accessed **2014** May, 21th.

(9) Prausnitz J. M.; Lichtenthaler R. N.; de Azevedo E. G. *Molecular Thermodynamics of Fluid-Phase Equilibria, Third edition*, Prentice Hall.**1998**, pp 191-195, 635-643.

(10) Yokozeki, A. *Int. J. Thermophys*. **2003,** *24*, 589-620.

(11) Huber, M.L.; McLinden, M.O.; Lemmon, E.W. *NIST Standard Reference Database 23, Reference Fluid Thermodynamic and Transport Properties-REFPROP, Version 8.0,* National Institute of Standards and Technology, Standard Reference Data Program, Gaithersburg, **2007**.

(12) Donnelly, H. G.; Katz, D. L. *Ind. Eng. Chem*. **1954**, *46*, 511‑517.

(13) Sterner, C. J. *Adv. Cryog. Eng*. **1961**, *6*, 467‑474.

(14) Davis, J. A.; Rodewald, N.; Kurata, F. *AIChE Journal*. **1962**, 8, 537-539

(15) Im, U. K.; Kurata, F. *J. Chem. Eng. Data*. **1971**, *16*, 295–299.

(16) Brewer, J.; Kurata, F. *AIChE Journal* **1958,** *4*, 317‑318.

(17) Boyle, G. J. *Shell Res. LTD*. Thornton Res. Centre P. O. Box. 1 Chester

(18) Cheung, H.; Zander, E.H.*Chem. Eng. Progr. Symp. Ser.* **1968**, *64*, 34-43.

(19) Streich, M. *Hydrocarbon Process* **1970**, *49*, 86-88

(20) Voss, G. *Diss. TU Berlin*, **1975**.

(21) Shen T.; Gao, T.; Lin W.; Gu A. *J. Chem. Eng. Data* **2012**, *57*, 2296−2303.

(22) Gao, T.; Shen T.; Lin W.; Gu A.; Ju Y. *Ind. Eng. Chem.* **2012**, 51, 9403‑9408.

(23) Pikaar, M. J. *Ph.D. Thesis*, University of London, London, **1959**.

(24) Agrawal, G. M.; Laverman, R. J. *Adv. Cryog. Eng*. **1974**,*19*, 327‑338.

(25) Le, T. T.;Trebble, M. A *J. Chem. Eng. Data* **2007**, 52, 683‑686.

(26) Zhang, L.; Burgass, R.; Chapoy, A.; Tohidi, B.; Solbraa, E. *J. Chem. Eng. Data* **2011**, *56*, 2971‑2975.

(27) Rodriguez-Reartes, S.B.; Cismondi, M.; Zabaloy, M.S. *J. of Supercritical Fluids* **2011**, *57*, 9–24.

(28) Yokozeki, A. *Int. J. Thermophys.* **2004**, *25*, 643–667.

(29) Stringari, P.; Campestrini, M. *Fluid Phase Equilib.* **2013**, *358*, 68–77.

(30) Stringari, P.; Campestrini, M.; Coquelet, C.; Arpentinier, P. *Fluid Phase Equilib.* **2014**, *362*, 258–267.

(31) Eggeman, T.; Chafin, S. *Chem. Eng. Prog*. **2005**, *101*, 39-44.

Table 1. Triple point and critical point pressure and temperature for CH_4 and CO_2.

Fluid	P_t / MPa	T_t / K	P_c / MPa	T_c / K
CH_4	0.011696	90.6941	4.5992	190.564
CO_2	0.517950	216.592	7.3773	304.1282

Table 2. Abbreviations used in Fig. 1 for the different kind of phase equilibria.

Abbreviation	Meaning
vle	vapor-liquid equilibrium curve (pure compound)
sle	solid-liquid equilibrium curve (pure compound)
sve	solid-vapor equilibrium curve (pure compound)
v=l	vapor-liquid critical locus (mixture)
$s_2$lve	solid$_2$-liquid-vapor equilibrium locus (mixture)
$s_1$lve	solid$_1$-liquid-vapor equilibrium locus (mixture)
$s_2s_1$le	solid$_2$-solid$_1$-liquid equilibrium locus (mixture)
$s_2s_1$ve	solid$_2$-solid$_1$-vapor equilibrium locus (mixture)

Table 3 Experimental data sources.

Author	Ref.	Kind of data	NEV	Molar fraction (x CO_2)	Temperature (K)	Pressure (MPa)
Donnelly and Katz	(12)	SLE	4	0.205-0.865	194.54-213.71	-
		SLVE	21	-	194.54-215.37	0.78-4.86
Sterner	(13)	SLVE	9	Liquid phase 0.019-0.052	166.48-199.82	1.95-4.97
Davis	(14)	SLVE	42	Liquid phase 0.0016-0.205	97.54-211.7	0.028-4.87
Im and Kurata	(15)	SLVE	10	Liquid phase: 0.006-0.175 Vapor phase: 0.0183-0.74	165.21-210.21	1.9-4.85
Brewer	(16)	SLE	8	0.18-1	190.37-215.37	-
Boyle	(17)	SLE	5	0.00027-0.00148	111.5-128	-
Cheung	(18)	SLE	9	0.0003-0.126	110.7-194.6	-
Streich	(19)	SLE	12	0.00031-1	110-218.3	-
Voss	(20)	SLE	22	0.0002-0.128	111.6-193.3	-
Shen et al.	(21)	SLE	9	0.000213-0.02896	112-169.9	0.093-2.315
Gao et al.	(22)	SLE	9	0.000172-0.02896	113.15-169.7	-
Pikaar	(23)	SVE	103	0.000265-0.59	132.65-210.15	0.156-4.832
Agrawall and Leverman	(24)	SVE	41	0.0012-0.11067	137.5-198	0.17-2.78
Le and Trebble	(25)	SVE	55	0.01-0.0293	168-187	0.96-3
Zhang et al.	(26)	SVE	17	0.108-0.54	196.5-210.3	0.29-4.45

Table 4. Coefficients of Eq. (6).

n_1	n_2	n_3	e_1	e_2	e_3
-1.47408	2.4327	-5.30618	1	1.9	2.9

Table 5. Values of the parameters in Eq. (8).

C_1 ($\times 10^{-9}$)	C_2 ($\times 10^{-6}$)	C_3 ($\times 10^{-6}$)
-1.0819	3.5919	4.2722

Table 6. Binary interaction parameters, k_{ij}, for the CH_4-CO_2 system.

	Model 1	**Model 2**
k_{ij}	0.11874	0.07

Table 7. AAD, Bias, and MAD% in calculating SLVE pressure at fixed temperature. Deviations are evaluated with respect to SLVE experimental pressures.

Ref	**AAD %**		**Bias %**		**MAD%**	
	Model 1	**Model 2**	**Model 1**	**Model 2**	**Model 1**	**Model 2**
(12)	13.77	12.23	-0.84	5.26	49.78	69.18
(13)	1.83	2.21	0.77	0.29	3.16	4.82
(14)	1.94	2.05	-0.82	-1.01	6.71	7.39
(15)	2.50	1.67	1.81	1.39	5.63	5.40
Overall	5.67	5.15	-0.30	1.40	49.78	69.18

Table 8. AAD, Bias, and MAD% obtained by comparison of the SVE temperatures calculated from Model 1 and 2 and the literature data. SVE temperatures have been calculated at fixed pressure and CO_2 molar fraction.

Ref	AAD %		Bias%		MAD%	
	Model 1	Model 2	Model 1	Model 2	Model 1	Model 2
(23)	0.53	0.47	-0.47	0.10	2.19	2.91
(24)	0.85	0.94	-0.20	0.46	2.02	2.49
(25)	1.60	1.29	-1.32	-0.73	3.67	2.96
(26)	0.40	0.44	-0.24	-0.01	0.98	1.31
Overall	0.85	0.77	-0.62	-0.06	3.67	2.96

Table 9. AAD, Bias, and MAD% obtained by comparison of the CO_2 molar fraction in the vapor phase of SVE calculated from Model 1 and 2 and the literature data. CO_2 molar fraction have been calculated at fixed pressure and temperature.

Ref	AAD %		Bias%		MAD%	
	Model 1	Model 2	Model 1	Model 2	Model 1	Model 2
(23)	8.88	7.13	7.92	-0.64	44.08	50.35
(24)	15.14	16.61	4.64	-6.57	41.61	44.21
(25)	31.49	24.69	27.26	16.31	80.59	64.09
(26)	5.84	5.54	3.78	-0.41	15.08	12.04
Overall	15.58	13.33	11.89	2.63	80.59	64.09

Table 10. AAD, Bias, and MAD% obtained by comparison of the SLE temperature calculated from Model 1 and 2 and the literature data. SLE temperatures have been calculated at fixed CO_2 molar fraction.

Ref	AAD%		Bias%		MAD%	
	Model 1	Model 2	Model 1	Model 2	Model 1	Model 2
(12)	1.77	1.08	0.76	0.58	4.58	3.31
(13)	2.53	3.71	-2.53	-3.71	4.22	5.21
(14)	1.65	1.67	-1.13	-1.67	2.29	3.00
(16)	0.64	1.03	-0.45	0.28	1.32	4.67
(17)	0.57	0.44	-0.55	0.11	1.17	0.83
(18)	1.90	2.20	-1.33	-1.84	3.75	3.47
(19)	2.17	1.78	1.63	1.04	4.04	2.84
(20)	1.92	2.34	-1.92	-2.33	3.14	3.74
(21)	2.27	2.47	-2.27	-2.47	2.83	3.28
(22)	2.37	2.58	-2.37	-2.58	4.71	4.39
Overall	1.84	1.98	-1.08	-1.36	4.71	5.21

Table 11. AAD, Bias, and MAD% obtained by comparison of the CO_2 molar fraction in the liquid phase of SLE calculated from Model 1 and 2 and the literature data. CO_2 molar fractions have been calculated at fixed temperature.

Ref	AAD%		Bias%		MAD%	
	Model 1	Model 2	Model 1	Model 2	Model 1	Model 2
(12)	22.74	16.88	-13.58	-11.78	41.54	37.26
(13)	29.37	40.45	29.37	40.45	51.13	63.61
(14)	17.89	16.43	11.89	14.26	30.99	29.86
(16)	14.51	11.11	2.01	-2.31	45.80	41.85
(17)	7.74	7.75	7.43	-6.36	15.54	14.03
(18)	25.89	24.27	20.24	18.00	62.69	44.41
(19)	23.34	23.86	-16.25	-17.13	53.80	49.96
(20)	23.36	23.52	22.26	22.44	46.11	41.08
(21)	30.40	25.65	30.40	25.65	42.00	34.38
(22)	34.47	28.83	34.47	28.83	99.26	70.09
Overall	23.28	21.82	14.23	12.51	99.26	70.09

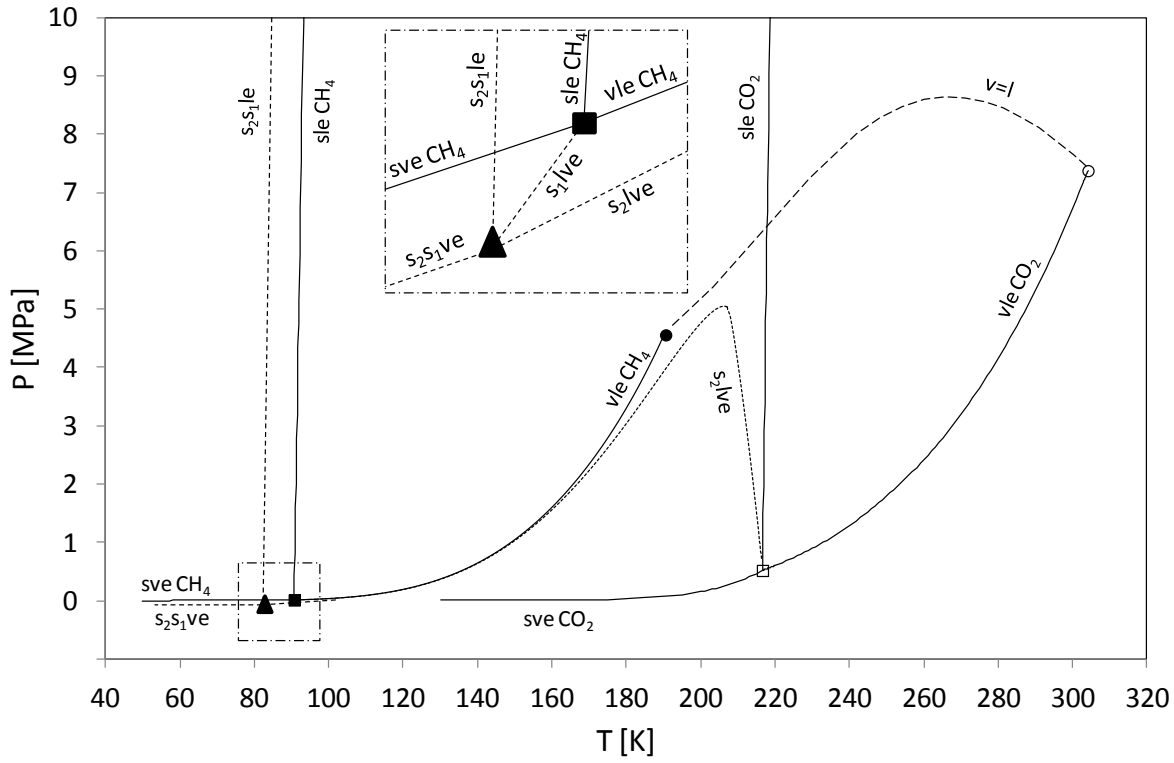

Figure 1. Pressure-temperature equilibrium behavior for the CH_4-CO_2 system: (■) CH_4 triple point; (●) CH_4 critical point; (□) CO_2 triple point; (○) CO_2 critical point; (▲) mixture quadruple point; (– –) vapor-liquid critical locus; (---) three-phase loci; (—) pure compound phase equilibria.

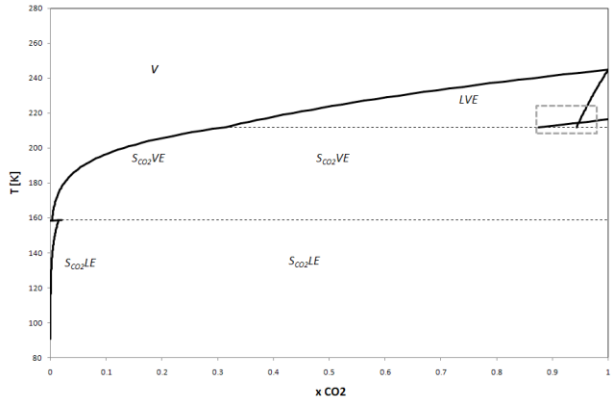

Figure 2. Phase diagram for CO_2-CH_4 mixture at 1.5 MPa. Solid lines: two-phase equilibrium lines; dotted lines: SLVE temperatures; dotted rectangle points out the inconsistency for the SLVE at the higher temperature. The same kind of inconsistency exists for the SLVE line at lower temperature, but it is not visible in the diagram.

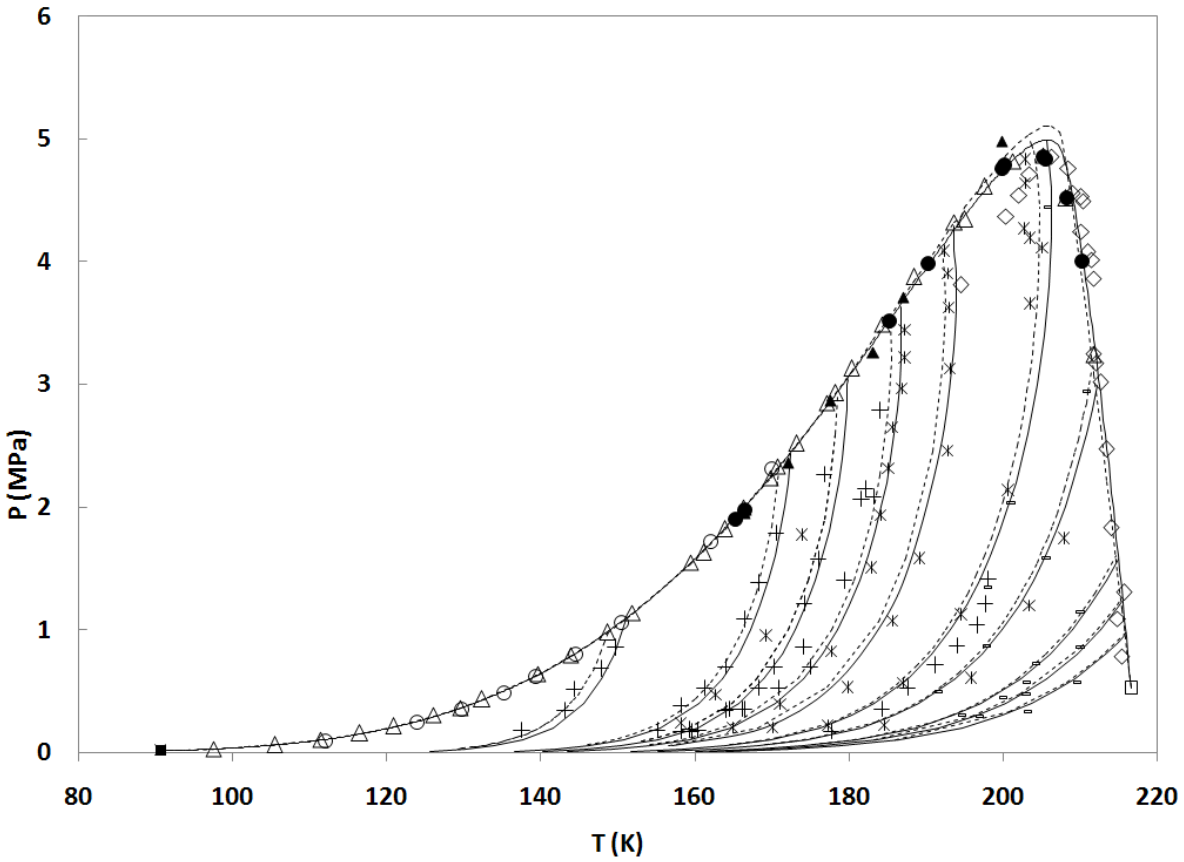

Figure 3. SLVE and SVE for the CH_4-CO_2 mixture. Experimental values; SLVE: (◊) Donnelly and Katz (12), (▲) Sterner (13), (Δ) Davis et al. (14), (●) Im and Kurata (15); (○) Shen et al.SLE data (21); SVE: (*) Pikaar (23), (+) Agrawal and Laverman (24), (-) Zhang et al. (26). Calculated values: (---) Model 1, (—) Model 2. (■) CH_4 triple point, (□) CO_2 triple point.SVE isopleths are at x_{CO2}=0.001, x_{CO2}=0.01, x_{CO2}=0.02, x_{CO2}=0.03, x_{CO2}=0.05, x_{CO2}=0.10, x_{CO2}=0.18, x_{CO2}=0.33, x_{CO2}=0.42, and x_{CO2}=0.54 from left to right.

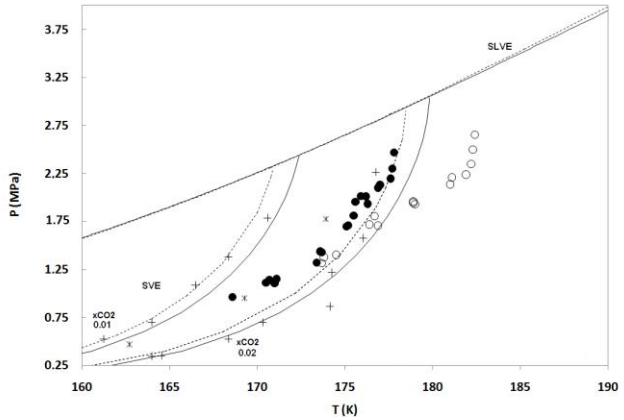

Figure 4. SLVE and SVE for the CH_4-CO_2 mixture. SVE isopleth at x_{CO2}=0.01, x_{CO2}=0.02; experimental values: Le and Trebble (25): (●) x_{CO2}=0.01 (21), (○) x_{CO2}=0.0191, (*) Pikaar (x_{CO2}=0.01) (23), (+) Agrawal and Laverman (x_{CO2}=0.01 and x_{CO2}=0.02) (24),. Calculated values: (---) Model 1, (—) Model 2.

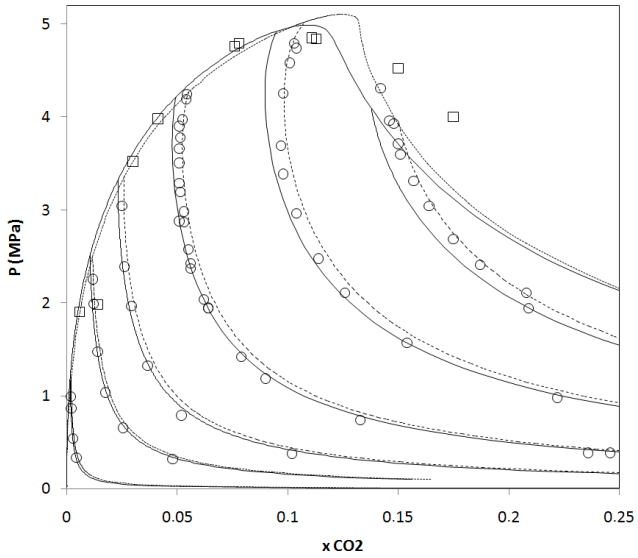

Figure 5. SVE at constant temperature for the CH_4-CO_2 mixture. (○) Experimental data from Pikaar (saturated cell data) (23) at 153, 173,183, 193, 203 and 210 K (from left to right); (□) triple point vapor composition data from Im and Kurata (15). Calculated values: (---) Model 1, (—) Model 2.

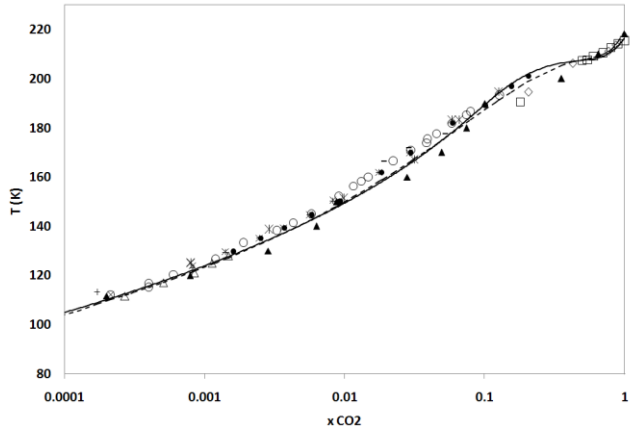

Figure 6. SLE for the CH_4-CO_2 mixture. Literature data: (◊) Donnelly and Katz (12); (-) Sterner (13); (●) Davis (14); (□) Brewer (16); (Δ) Boyle (17); (*) Cheung (18); (▲) Streich (19); (○) Voss (20); (×) Shen et al. (21); (+) Gao et al. (22);. Calculated values: (---) Model 1, (—) Model 2.